Multi-scale evaluation of the linear elastic and failure parameters of the unidirectional laminated textiles with application to transverse impact simulation

CrossMark

D. Calneryte *, R. Barauskas

Department of Applied Informatics, Faculty of Informatics, Kaunas University of Technology, Studentu St. 50-407, LT-51368 Kaunas, Lithuania

A B S T R A C T

Unidirectional laminated textiles (UDLTs) are flexible non-crimped fabric structures, the UD layers of which are bonded together by small amounts of thermoplastic resin and covered by polyethylene films over their external surfaces. Applications of them in ballistic protection clothes ensure lesser costs and ability to resist the penetration of humidity, which may substantially decrease the overall ballistic strength of the structure. This research focuses on the hierarchical multi-scale approach formulated for large displacement, material non-linearity and failure. The micro-scale model of UDLT represents matrix and fibres by means of 3D solid elements. A representative small volume (micro-cube) of the UDLT composite is subjected to a series of large deformation tests up to the failure, which enable to approximately evaluate linear elastic and failure parameters of the orthotropic shell elements that represent the mechanical behaviour of UDLT at rougher scale. Obtained longitudinal, transversal and shear strength parameters in association with the corresponding strains are the parameters used at mezzo-scale in order to calculate the Hashin criteria for the shell element failure. The results of the research are employed in order to achieve reasonable computational costs during the simulation of ballistic penetration through multi-layer UD composite textile structures at medium velocity range.

© 2016 Elsevier Ltd. All rights reserved.

1. Introduction

Composite textiles consist of several materials with significantly different properties. Usually the material with low stiffness and therefore marked shear flexibility is reinforced with particles or fibres of much higher stiffness. Moreover, the properties of composites also depend on the length and distribution of reinforcing fibres. We focus on the unidirectional fibre composites in this research. Unidirectional composite textile consists of long fibres aligned in one direction, which are bonded together by the matrix material. The advantages of unidirectional composite fabrics are light weight (low density), high strength in the longitudinal direction, high impact strength and high strength-to-weight ratio. UDLT are widely used to manufacture lightweight high stiffness and strength products such as helmets, bullet-proof vests, aircraft parts etc.

Due to the complex internal micro-structure of UDLT, the simulation models of transverse impact on it are developed by employing multi-scale approaches. The multi-scale approach enables to simulate the structure by means of rougher models and simultaneously to retain all main features of the mechanical behaviour of the material. Most often two or three-scale model representations are applied. By using two-scale (micro-macro) approaches the internally multi-layer and multi-directional volumes of a composite structure may be presented by continuous shell or volumetric finite elements, where the equivalent properties of the material are obtained by investigating the characteristic behaviour of the selected representative volume element (RVE) of the composite. Within the RVE, the internal geometrical structure of the composite is represented as detailed as appropriate, by taking into account real possibilities of the simulation software employed for the analysis. Three-scale approaches introduce an intermediate scale (mezzo-scale), which still represents the most important formations of the modelled object by including them directly into the patterns of the finite element structure. However, the geometric patterns in the mezzo-scale are much more generalised and rougher compared against the micro-scale representations. As an example, the multi-filament yarns of the woven textiles presented by shell or solid elements is a typical example of the mezzo-scale, as they enable to represent explicitly the patterns of the weave including the contact interactions among the

yarns [1–3]. The micro-scale model is employed for determining the material properties of the elements, which represent the yarn, while the corresponding macro-scale model presents the woven structure as continuous membrane, the properties of which are obtained by investigating the mechanical behaviour of the mezzo-level structure. In case of UDLT, the mezzo-scale represents a single UD layer by shell elements, while in the micro-level we tend to fully investigate the geometric pattern of the filaments and matrix material in contained in the RVE of the UD layer. In the mezzo-level multi-layer, multi-directional and multi-sheet textile structures are composed of UD layer shell elements by taking into account possible contact interactions, sliding and friction between adjacent layers. At the macro-level the multi-layer textile composite may be represented as orthotropic membrane, the properties of which are established by analysing the characteristic portion of the corresponding mezzo-scale model.

In the range of small displacements and linear behaviour of the material the usual approach is to compute the relation between the means of the stresses and strains over the statistically representative sample of material referred as a representative volume element (RVE) and to apply the effective properties in the macro scale. Another approach for evaluation of effective linear elastic material constants discussed in [4] was based on the analytical micromechanical models (direct and modified rules of mixture) and finite element (FE) modelling. Longitudinal, transverse and shear strengths of the UDLT could be evaluated by considering fibre shapes and their distribution [5], analytically or numerically. A generalised three-scale model was proposed in [6] for prediction of the strength of weaved, braided, stitched or knitted textiles, where material heterogeneities were modelled as a unit cell of UDLT with periodic boundary conditions in micro-scale. The homogenised parameters and stress–strain curves were obtained by using FE analysis. Similarly, the periodic boundary conditions were applied to RVE of hexagonal array in order to obtain the stress–strain curves by means of explicit FE analysis in [7]. The appropriate boundary conditions applied on the RVE of UDLT in each loading case were discussed in [8]. In case the fibres of the UDLT are aligned perfectly and the structure is periodic, the RVE is a unit cell of either hexagonal, diamond or square array [8,9]. Random defects can be considered by means of the RVE, which includes all microstructural heterogeneities that occur in the composite [10].

The aim of this research is to numerically evaluate the effective linear elastic and failure parameters of the unidirectional laminated textile (UDLT) by investigating large strains and stresses of the RVE. The main issue is to clarify if the failure conditions obtained from RVE analysis in the micro-scale can be directly applied for establishing the failure criteria of the equivalent model in rougher scale. The transition from micro to UD layer shell element at mezzo-level is performed by investigating the characteristic behaviour of the RVE of the composite material.

Low density polyethylene matrix reinforced with aramid fibres was used as a sample material combination in the micro-scale. Aramid is an important reinforcement material due to its high tensile strength and high stiffness, low density, resistance to high temperature and other useful properties [11]. Two kinds of FE models were used in this investigation. The micro-scale model assembled of solid elements represents the internal micro-structure of the UDLT and is computationally expensive. The RVE of this model was used to evaluate the relation between stresses and strains of the UDLT under the pure strain constraints. However, if pure shear is modelled with the assumption that the deformed RVE remains parallelogram with straight edges, the obtained shear moduli may depend on the size of the analysed RVE. This assumption is an overly restrictive constraint and the deformed RVE needs to satisfy only periodicity and symmetry conditions for the pure shear modelling [8]. These conditions were taken into account for modelling pure shear strains. The implicit FE analysis is employed to obtain linear elastic parameters such as Young's moduli in longitudinal and transverse directions, Poisson's ratio and shear moduli. The explicit FE analysis with slowly increasing displacements is employed to obtain failure parameters such as longitudinal and transverse tensile strengths, shear strength and respective strains. The Hashin failure criterion is employed in shell elements of the UD layer. This research may be considered as a further development of our recent work [12], where the UDLT plies subjected to ballistic impact were presented by three-zone FE models constructed at different scales. The known longitudinal failure strains of aramid fibres were directly used for the representation of the damage, however, a very important role was devoted for proper erosion strain values used in the model. It was demonstrated that proper combinations of failure and element erosion strains could be established for the models of certain refinement range and worked quite well, however, this lacked a solid theoretical background. The development in this work tends to establish these values at the level of RVE, as well as, convergence issues are considered. The numerical experiments of the sphere impacting solid and shell models are compared to adjust the erosion value of shell model.

Although misaligned fibres and other defects can occur during the manufacturing process, the material model with perfectly aligned fibres is analysed in this research. Moreover, it is assumed that the contact between the matrix and fibre system is perfect. The interface between matrix and fibre should be added otherwise [13].

2. Multiscale model

The multiscale model "bottom-to-top" was applied in this research. The internal structure of the UD layer of the composite layer and the properties of its materials are known in the micro-scale. The structure analysed in the micro-scale is assumed to be ideally periodic with square filling of the fibres. All fibres have square arrangements without any overlapping. The unit cell of the micro-level model consists of a cylindrical aramid fibre inserted into the cubic volume of the low density polyethylene matrix (Fig. 1). This type of the unit cell corresponds to square fibre distribution in the UDLT and can be applied for the composites if the filling does not exceed 78.5%. The hexagonal type of the structure should be used otherwise [7].

The stress–strain relation of the aramid fibre is almost linear until the failure (Fig. 2(a)). The matrix material, on the contrary, is elastic for small deformation only and undergo large plastic deformations (Fig. 2(b)).

The *MAT_PLASTIC_KINEMATIC material model (MAT_003) is employed in LS-DYNA to model the fibre and matrix materials with parameters in Table 1. This material model enables to simulate the failure of elements by defining the erosion strain value.

Model analysed in the mezzo scale is a small fragment of a macro model and represents the most important formations of the modelled object such as number of unidirectional layers and material properties of each layer that depend on the direction of fibres. Moreover, the interaction between the adjacent layers is considered in this scale. The layer of the unidirectional fibre composite in the mezzo scale is simulated using material model *MAT_LAMINATED_COMPOSITE_FABRIC (MAT_58). This model may be used to simulate composite materials with unidirectional layers, complete laminates and woven fabrics [14]. The failure surface type FS = 0 appropriate for unidirectional composites is applied in calculations. Linear elastic parameters, strength points with respective strains and erosion strain for this material model are evaluated using RVE in the micro-scale.
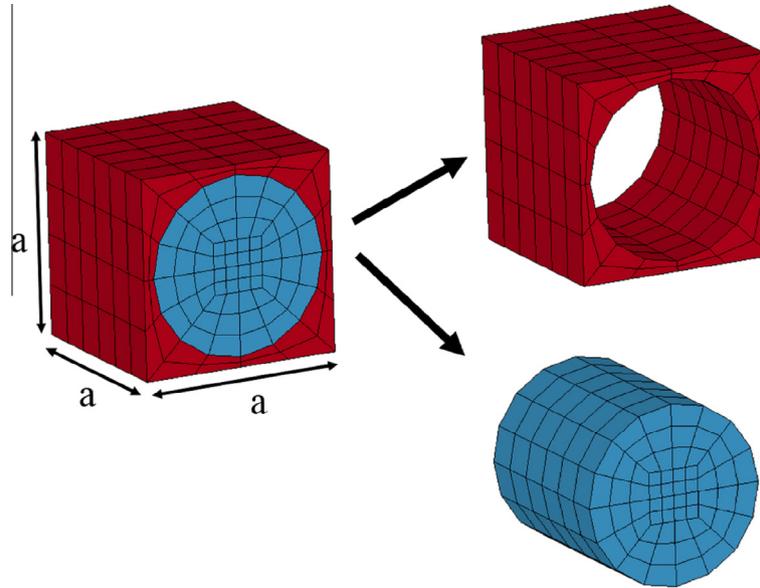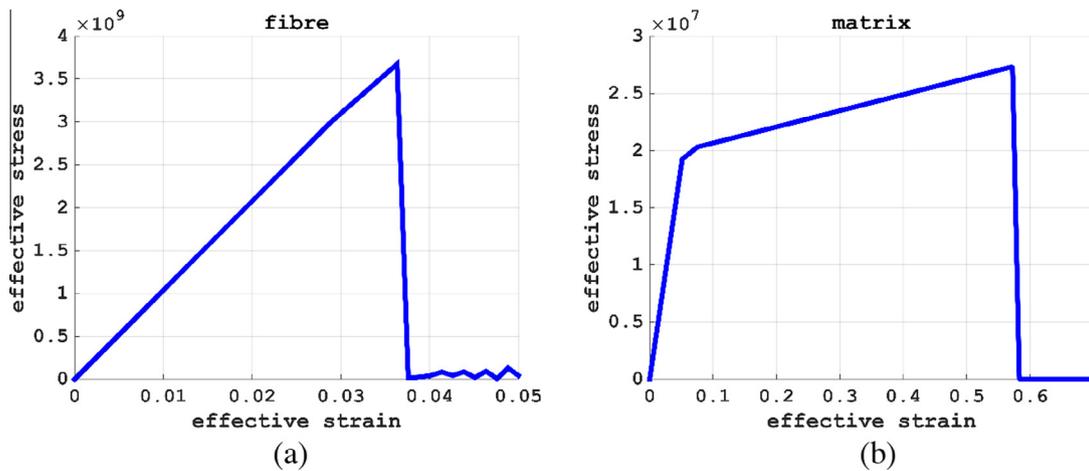
Fig. 1. Scheme of RVE.

Fig. 2. Effective stress–effective strain curves for the fibre (a) and matrix (b).

Table 1
Mechanical constants of fibre and matrix material.

	Fibre	Matrix
Young's modulus	9E+010 N/m²	3E+08 N/m²
Poisson's ratio	0.3	0.2
Yield stress	2E+07 N/m²	3.5E+09 N/m²
Mass density	1400 kg/m³	920 kg/m³
Effective strain at failure	0.036	0.5

2.1. Evaluation of linear elastic parameters of UDTL

Homogenisation is based on analysing the material structure in the micro-scale. The fibre direction coincides with X axis. The RVE of UDLT is employed for obtaining the homogenised mechanical stiffness constants by performing the FE analysis. The method described in [12] is applied to calculate stiffness tensor for small strains. The six pure strains are created for the RVE by prescribing the necessary displacements on the sides of the RVE in accordance with the schemes in (Fig. 3). For the pure longitudinal strain (loading case I) the small displacements δ are prescribed for the nodes

on the front face of the RVE ($x = a$). Displacements of other faces of the RVE are constrained in normal directions as:

$$I : \quad u(a, y, z) = \delta, \quad u(0, y, z) = 0, \quad v(x, 0, z) = v(x, a, z) = 0,$$
$$w(x, y, 0) = w(x, y, a) = 0 \tag{1}$$

where $u(x, y, z)$, $v(x, y, z)$, $w(x, y, z)$ denote displacements in X, Y and Z directions respectively. Similarly, the pure strains in the transverse Y (II) and Z (III) directions are simulated by imposing the displacements of RVE faces as:

$$II : \quad u(0, y, z) = u(a, y, z) = 0, \quad v(x, a, z) = \delta, \quad v(x, 0, z) = 0,$$
$$w(x, y, 0) = w(x, y, a) = 0 \tag{2}$$

$$III : \quad u(0, y, z) = u(a, y, z) = 0, \quad v(x, 0, z) = v(x, a, z) = 0,$$
$$w(x, y, a) = \delta, \quad w(x, y, 0) = 0 \tag{3}$$

The pure shear strains (loading cases IV, V and VI for shear strains XY, YZ, ZX respectively) are simulated by prescribing the displacements of the nodes at the faces of the RVE with periodic boundary conditions:
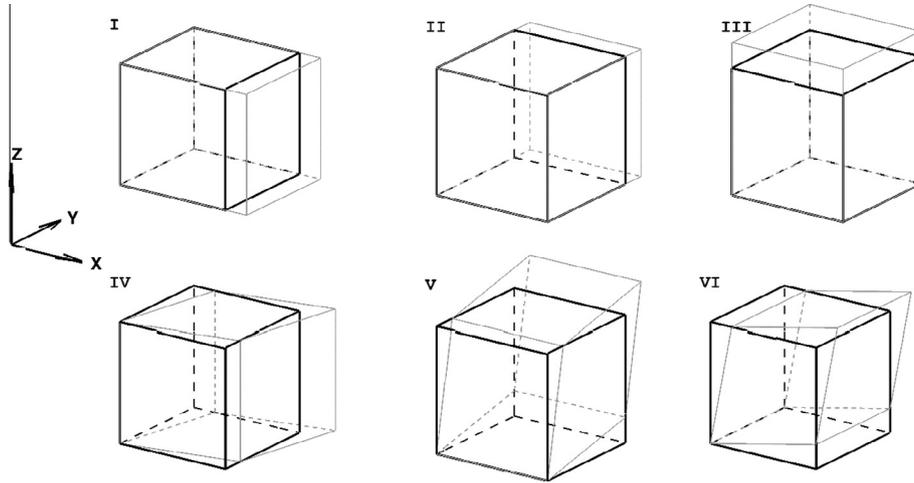
Fig. 3. Schemes for creating pure strains: I – longitudinal strain mode; II, III – transverse strain mode; IV, V, VI – shear strain mode in *XY*, *YZ*, *ZX* plane respectively.

$\text{IV} : u(x, a, z) = \delta, \quad u(0, y, z) = u(a, y, z), \quad v(a, y, z) = \delta,$

$v(x, 0, z) = v(x, a, z), \quad w(x, y, 0) = w(x, y, a) = 0 \qquad (4)$

$\text{V} : u(0, y, z) = u(a, y, z) = 0, \quad v(x, y, a) = \delta,$

$v(x, 0, z) = v(x, a, z), \quad w(x, a, z) = \delta, \quad w(x, y, 0) = w(x, y, a) \qquad (5)$

$\text{VI} : u(x, y, a) = \delta, \quad u(0, y, z) = u(a, y, z),$

$v(x, 0, z) = v(x, a, z) = 0, \quad w(a, y, z) = \delta, \quad w(x, y, 0) = w(x, y, a) \qquad (6)$

The effective stiffness tensor is valid for small strains only and is obtained by linear relation of mean stresses over RVE and strains:

$$\mathbf{C} = \begin{bmatrix} \sigma_x^\mathrm{I} & \sigma_x^\mathrm{II} & \sigma_x^\mathrm{III} & \sigma_x^\mathrm{IV} & \sigma_x^\mathrm{V} & \sigma_x^\mathrm{VI} \\ \sigma_y^\mathrm{I} & \sigma_y^\mathrm{II} & \sigma_y^\mathrm{III} & \sigma_y^\mathrm{IV} & \sigma_y^\mathrm{V} & \sigma_y^\mathrm{VI} \\ \sigma_z^\mathrm{I} & \sigma_z^\mathrm{II} & \sigma_z^\mathrm{III} & \sigma_z^\mathrm{IV} & \sigma_z^\mathrm{V} & \sigma_z^\mathrm{VI} \\ \tau_{xy}^\mathrm{I} & \tau_{xy}^\mathrm{II} & \tau_{xy}^\mathrm{III} & \tau_{xy}^\mathrm{IV} & \tau_{xy}^\mathrm{V} & \tau_{xy}^\mathrm{VI} \\ \tau_{yz}^\mathrm{I} & \tau_{yz}^\mathrm{II} & \tau_{yz}^\mathrm{III} & \tau_{yz}^\mathrm{IV} & \tau_{yz}^\mathrm{V} & \tau_{yz}^\mathrm{VI} \\ \tau_{zx}^\mathrm{I} & \tau_{zx}^\mathrm{II} & \tau_{zx}^\mathrm{III} & \tau_{zx}^\mathrm{IV} & \tau_{zx}^\mathrm{V} & \tau_{zx}^\mathrm{VI} \end{bmatrix} \cdot \begin{bmatrix} \varepsilon_x^\mathrm{I} & & & & & \\ & \varepsilon_y^\mathrm{II} & & & & \\ & & \varepsilon_z^\mathrm{III} & & & \\ & & & \gamma_{xy}^\mathrm{IV} & & \\ & & & & \gamma_{yz}^\mathrm{V} & \\ & & & & & \gamma_{zx}^\mathrm{VI} \end{bmatrix}^{-1}$$

$$(7)$$

where superscript indicates the loading case, σ and τ are the means longitudinal and shear stresses, ε and γ are the longitudinal and shear strains of RVE. The mean stresses are calculated as a weighted mean over the elements in RVE:

$$\sigma = \sum_{i=1}^{N} \frac{V_i}{V} \sigma^i, \sigma^i = \begin{bmatrix} \sigma_x^i & \sigma_y^i & \sigma_z^i & \tau_{xy}^i & \tau_{yz}^i & \tau_{zx}^i \end{bmatrix}^T \qquad (8)$$

where V_i is volume of the *i*th element and V is the volume of the RVE.

The effective linear elastic parameters of material model for the shell element are defined by longitudinal and transverse Young's moduli (E_x, E_y, E_z), Poisson's ratio in the shell plane (v_{yx}) and shear moduli (G_{xy}, G_{yz}, G_{zx}). All these parameters are obtained from the compliance matrix **S** which is inverse of **C** and has a form:

$$\mathbf{S} = \begin{bmatrix} \frac{1}{E_x} & -\frac{v_{yx}}{E_y} & -\frac{v_{zx}}{E_z} & 0 & 0 & 0 \\ -\frac{v_{xy}}{E_x} & \frac{1}{E_y} & -\frac{v_{zy}}{E_z} & 0 & 0 & 0 \\ -\frac{v_{xz}}{E_x} & -\frac{v_{yz}}{E_y} & \frac{1}{E_z} & 0 & 0 & 0 \\ 0 & 0 & 0 & \frac{1}{G_{xy}} & 0 & 0 \\ 0 & 0 & 0 & 0 & \frac{1}{G_{yz}} & 0 \\ 0 & 0 & 0 & 0 & 0 & \frac{1}{G_{zx}} \end{bmatrix} \qquad (9)$$

where $\frac{v_{xy}}{E_x} = \frac{v_{yx}}{E_y}, \frac{v_{yz}}{E_y} = \frac{v_{zy}}{E_z}, \frac{v_{zx}}{E_z} = \frac{v_{xz}}{E_x}$.

2.2. Evaluation of failure parameters (strength)

The failure of shell elements can be defined by several criteria such as maximum stress, maximum strain, Hill–Tsai, Hashin and others. General formulation of failure criteria applied to evaluate loads that cause failure of the individual layer of the unidirectional composite is described in [5]. Failure criteria for the shell element is described specifying the combination of stresses in local axes that cause fracture:

$$F(\sigma_x, \sigma_y, \tau_{xy}) = 1 \qquad (10)$$

where σ_x, σ_y stresses in longitudinal and transverse directions of the composite and τ_{xy} is shear stress. This means that shell element works without failure if $F < 1$, fails if $F = 1$ and is failed if $F > 1$.

The Hashin failure criterion is applied to simulate the failure of the individual layer of the shell for the material model used in numerical experiments. This criteria predicts failure in longitudinal (fibre tension and compression) and transverse (matrix tension and compression) modes [15]:

- Fibre tension and compression:

$$\left(\frac{\sigma_x}{XX}\right)^2 - 1 = \begin{cases} \geqslant 0, & failed \\ < 0, & elastic \end{cases} \qquad (11)$$

where $XX = \begin{cases} XT, & \text{if} \quad \sigma_x \geqslant 0 \\ XC, & \text{if} \quad \sigma_x < 0 \end{cases}$, XT, XC – longitudinal tensile and compressive strengths, X axis coincides with the fibre direction.

- Matrix tension and compression:

$$\left(\frac{\sigma_y}{YY}\right)^2 + \left(\frac{\tau_{xy}}{SC}\right)^2 - 1 = \begin{cases} \geqslant 0, & failed \\ < 0, & elastic \end{cases} \qquad (12)$$

where $YY = \begin{cases} YT, & \text{if} \quad \sigma_y \geqslant 0 \\ YC, & \text{if} \quad \sigma_y < 0 \end{cases}$, YT, YC – transverse tensile and compressive strengths, SC – shear strength.

The stiffness and strength of the UD composite in the longitudinal direction are governed by the stiffness and strength of fibres. Assume the stress–strain curves of aramid composites under the longitudinal tension are close to linear until the failure. The stiffness and strength of the UD composite in the transverse direction and under the shear load are influenced by both matrix and fibre materials. Usually the damage under the transverse tensile or shear load occurs in the matrix, fibre–matrix interface or fibre failure if fibres consist of thin filaments and therefore have low transverse strength [5,16]. The explicit FE analysis of the RVE is

employed in order to obtain the failure limits of the UD composite. The prescribed displacements are increased linearly till the failure of the matrix or of the fibres takes place. The failure of the laminated composite material model is defined by longitudinal and transverse tensile strengths *XT*, *YT* and shear strength *SC* with the respective failure strains ε_{XT}, ε_{YT}, γ_{SC}. These values are obtained from the true stress–true (Hencky) strain curves under the longitudinal transverse and shear loading (Fig. 4). The true strain tensor is determined as [12]:

$$\boldsymbol{\varepsilon}^H = \frac{1}{2} \cdot \log\left(\mathbf{I} + 2 \cdot \boldsymbol{\varepsilon}^G\right) = \frac{1}{2} \cdot \log\left(\mathbf{F}^T \cdot \mathbf{F}\right) \tag{13}$$

where **I** is identity matrix, $\boldsymbol{\varepsilon}^G$ is Green's strain tensor, **F** is a deformation gradient tensor:

$$\mathbf{F} = \begin{bmatrix} 1 + \frac{\partial u}{\partial x} & \frac{\partial u}{\partial y} & \frac{\partial u}{\partial z} \\ \frac{\partial v}{\partial x} & 1 + \frac{\partial v}{\partial y} & \frac{\partial v}{\partial z} \\ \frac{\partial w}{\partial x} & \frac{\partial w}{\partial y} & 1 + \frac{\partial w}{\partial z} \end{bmatrix} \tag{14}$$

where *u*, *v*, *w* are displacements in *X*, *Y* and *Z* directions.

As the maximum stress criterion is applied to identify the strength of the material model in the micro-scale, the parameters *XT*, *YT* and *SC* are maximum longitudinal, transverse and shear stresses reached before the failure under the longitudinal, transverse and shear loading respectively:

$$XT = \max_t\left(\sigma_x^{[t]}\right); \quad \varepsilon_{XT} = \varepsilon_x^{[t']}, \quad t' : \sigma_x^{[t']} = XT \tag{15}$$

$$YT = \max_t\left(\sigma_y^{[t]}\right); \quad \varepsilon_{YT} = \varepsilon_y^{[t']}, \quad t' : \sigma_y^{[t']} = YT \tag{16}$$

$$SC = \max_t\left(\tau_{xy}^{[t]}\right); \quad \gamma_{SC} = \gamma_{xy}^{[t']}, \quad t' : \tau_{xy}^{[t']} = SC \tag{17}$$

Thus, the pairs (ε_{XT}, XT), (ε_{YT}, YT) are the points of tensile stress–strain curves at which the failure in particular direction is expected [12]. The shear failure is expected at the point (γ_{SC}, SC) under shear loading. The pairs (ε_{XC}, XC), (ε_{YC}, YC) define compressive failure points and are assumed to be equal to the tensile strengths and strains in numerical examples. As the strength point is reached, the respective stress of shell element is reduced to the fixed value
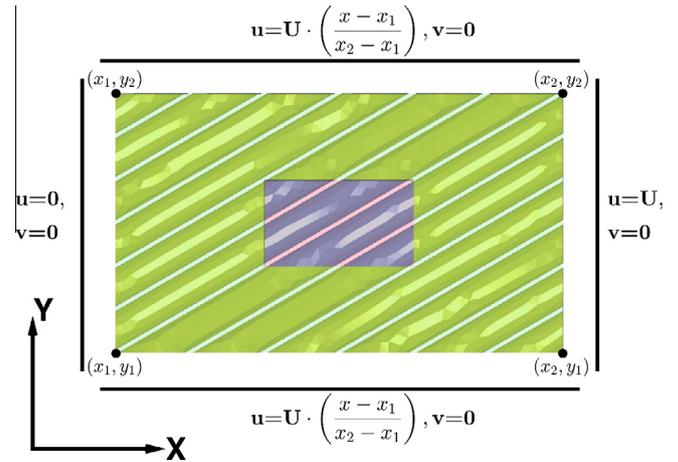

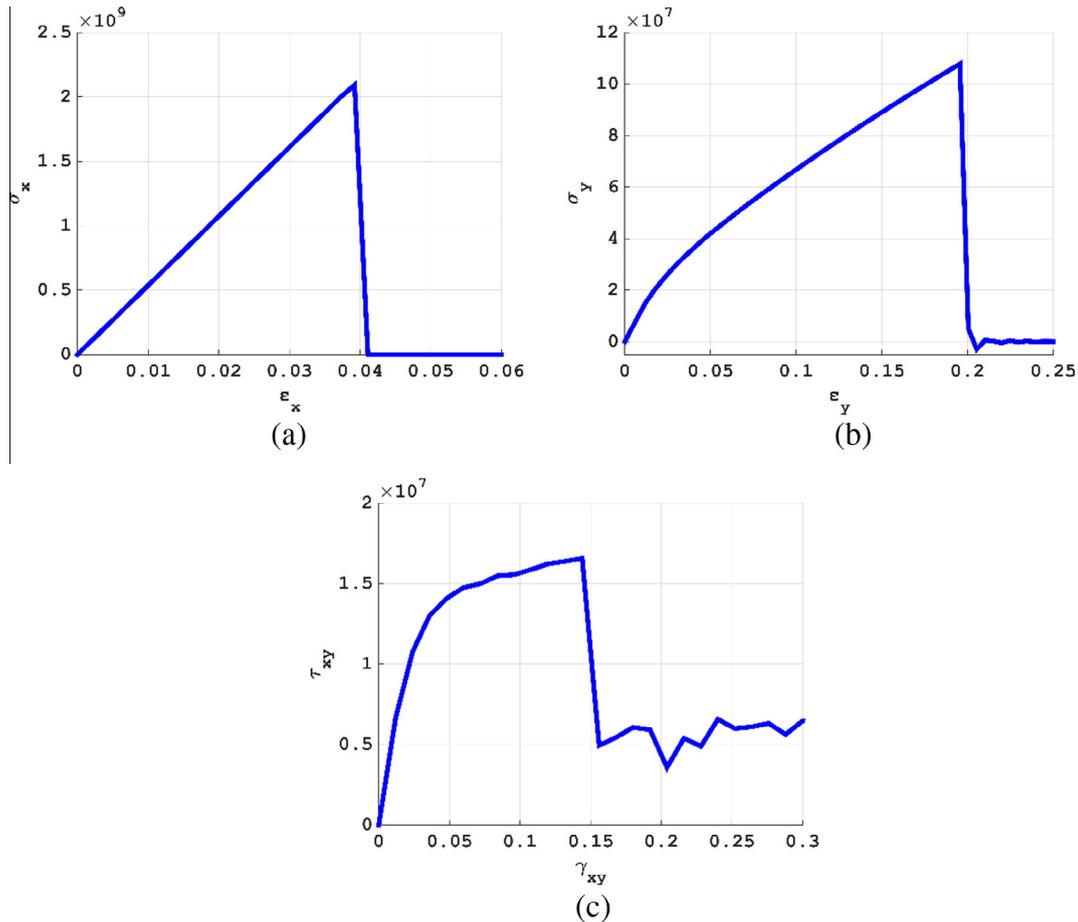**Fig. 5.** Boundary conditions for ERODS evaluation.

Fig. 4. Stress–strain curves of the RVE for the strength evaluation in longitudinal tensile mode (a); transverse tensile mode (b); XY shear mode (c).
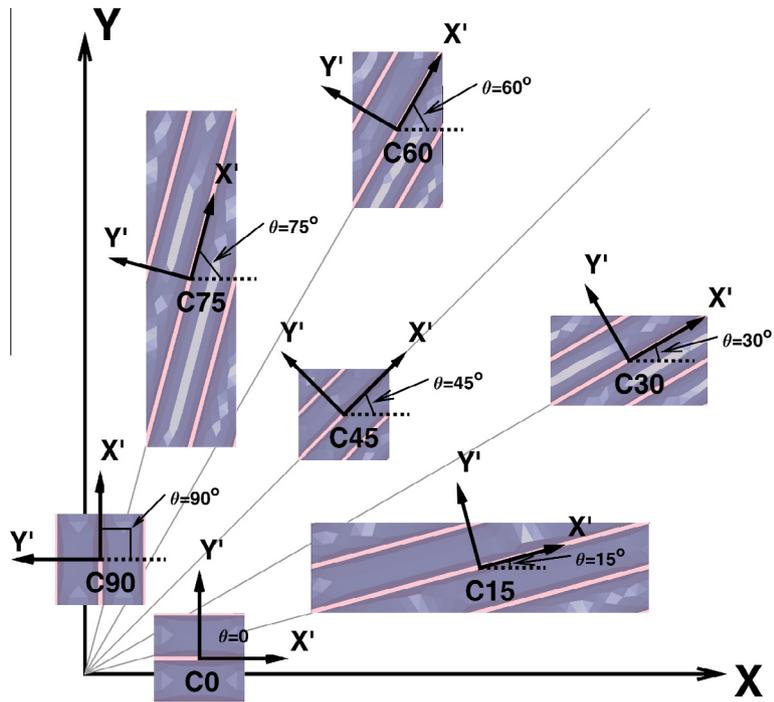
Fig. 6. Analysed models for the ERODS evaluation in coordinate system (X–Y–Z) with material coordinate system (X'–Y'–Z). Axis Z coincides for both coordinate systems.
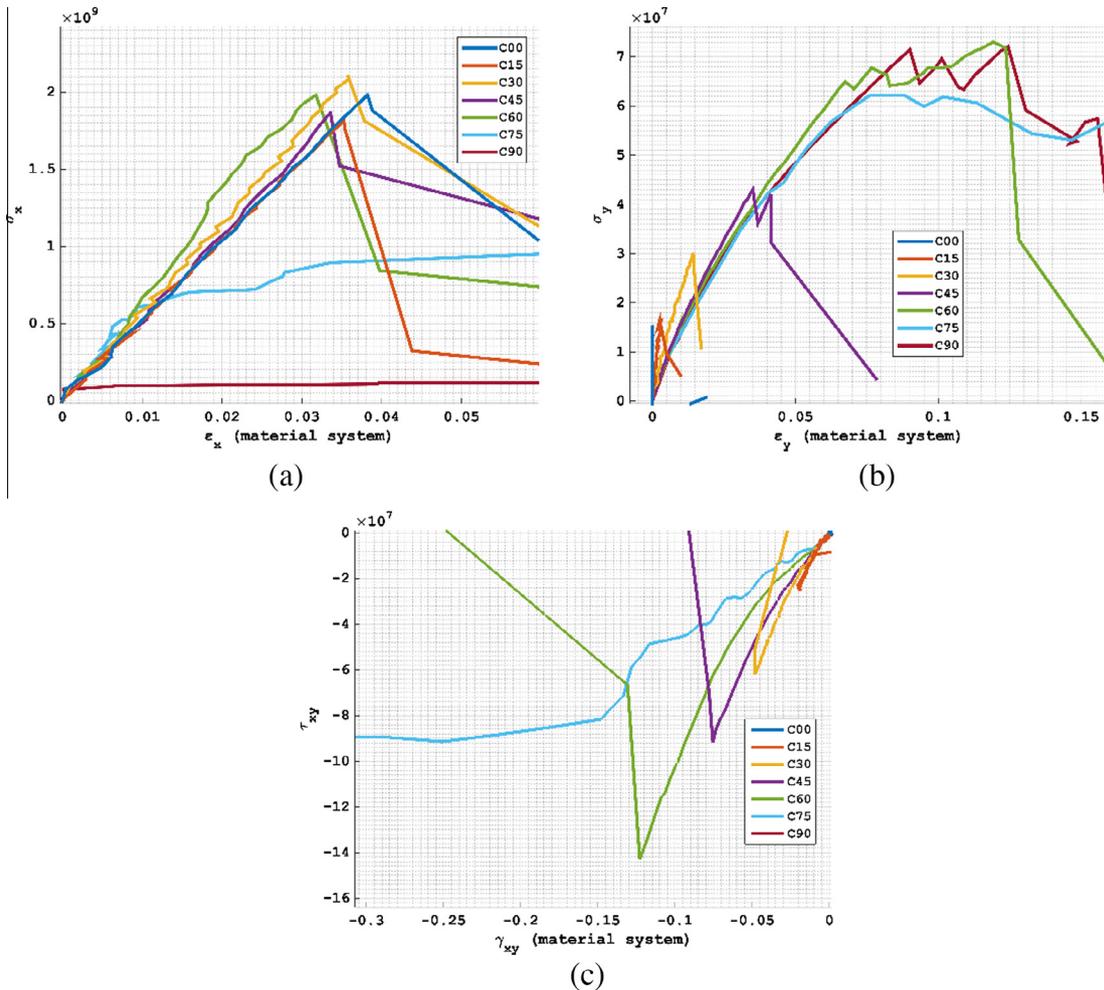

Fig. 7. Stress strain curves of the models: longitudinal (a); transverse (b); shear (c) in the material coordinate system.

Table 2
ERODS values applied in numerical examples.

	C00	C15	C30	C45	C60	C75	C90
ERODS	0.045	0.049	0.078	0.118	0.231	0.919	5

but the element retains its strength in other directions. For example, if shell element reaches its strength point in longitudinal (fibre) direction, the longitudinal stress is reduced to small value but the element exhibits elastic stress–strain behaviour in transverse direction and shearing. This is a contradiction to the solid element model where the RVE fails completely if the fibres of the analysed model fail. Moreover, the shell element remains in the structure and continues to deform even though all strength points are reached. In addition, such elements increase stiffness of the structure in contact problems.

2.3. Evaluation of erosion strain

The different conditions for the deletion of shell element can significantly change the stiffness of the structure in contact problems. The shell element in LS-DYNA is deleted if the maximum effective strain defined by parameter ERODS is reached. The effective strain ES combines longitudinal, transverse and shear strains in the material coordinate system:

$$ES = \frac{2}{\sqrt{3}} \sqrt{3 \cdot \left(\frac{\varepsilon_x + \varepsilon_y}{2}\right)^2 + \left(\frac{\varepsilon_x - \varepsilon_y}{2}\right)^2 + \gamma_{xy}^2} \qquad (18)$$

The UDLT is considered as failed if the fibres of the structure fail. This determines that ERODS should be equal to the strain value at longitudinal strength point ε_{XT} for the shell element under the longitudinal tension. However, this ERODS value results in inadequately low stiffness of the structure in the mezzo model where the strains are combined. Similarly to the previous example, the fibres do not fail under the transverse tensile loading and the ERODS value for the elements under this type of loading should be equal to infinity. In case of large ERODS values, the stiffness of mezzo model is overrated and elements undergo unrealistically large deformations.

To define the ERODS value, the RVE should exhibit combined strains. These conditions are created by prescribing gradually increasing displacements U according the scheme in Fig. 5 for the material sample rotated by angle θ. The sample intends to fail in the middle zone and the failure strain of the marginal zone is significantly higher in order to avoid the material failure caused by the prescribed artificial displacements. Material samples analysed in this research are shown in Fig. 6 with the respective material coordinate system. The samples maintain periodicity and include all heterogeneities of the rotated micro-structure. This results in different sizes of samples.
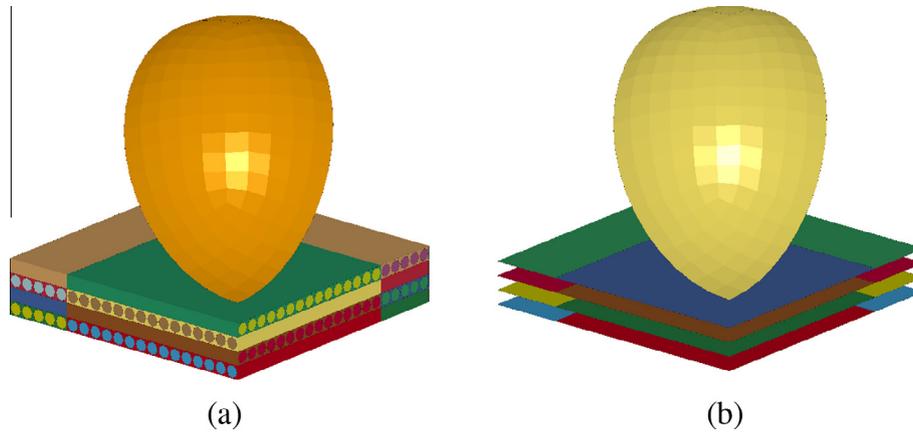

Fig. 8. Solid element model (a) and shell element model (b) of 4 crossed plies in contact with rigid sphere.

Table 3
Mechanical constants of homogeneous unidirectional ply in the material plane (*a,b,c*) where *a* axis coincides with the fibre direction, *b* axis corresponds to the transverse direction and *c* axis corresponds to the shell thickness direction.

Ea	Longitudinal Young's modulus	5.344e10 N/m²
Eb	Transverse Young's modulus	1.2519e9 N/m²
Pba	Poisson's ratio, ba plane	0.006205
Gab	Shear moduli corresponding to planes ab, bc, ca	5.61e8 N/m²
Gbc		4.5047e8 N/m²
Gca		5.61e8 N/m²
	Mass density	1200 kg/m³
Non-linear and failure constants		
XC, XT	Longitudinal compressive and tensile strength	2.0919e9 N/m²
YC, YT	Transverse compressive and tensile strength	1.07819e8 N/m²
SC	Shear strength	1.656e7 N/m²
E11C, E11T	Strain at longitudinal compressive and tensile strength	0.03922
E22C, E22T	Strain at transverse compressive and tensile strength	0.19557
GMS	Strain at shear strength	0.144
SLIMS	Shear stiffness reduction coefficient	0.1
SLIMTi	Tensile stiffness reduction coefficient	0.1
SLIMCi	Compressive stiffness reduction coefficient	1

Table 4
Mechanical constants of rigid sphere.

Young's modulus	1.7E+010 N/m^2
Poisson's ratio	0.4
Mass density	11,270 kg/m^3

The mean stress–strain relations are calculated for the middle zone in the global coordinate system. As the ERODS is defined with respect to the direction of the fibres, the calculated stress and strain values are transferred to the material coordinate system (X', Y', Z') using the standard transformation:

$$\begin{bmatrix} \sigma_{x'} & \tau_{x'y'} & \tau_{x'z'} \\ \tau_{y'x'} & \sigma_{y'} & \tau_{y'z'} \\ \tau_{z'x'} & \tau_{z'y'} & \sigma_{z'} \end{bmatrix} = \mathbf{T} \begin{bmatrix} \sigma_x & \tau_{xy} & \tau_{xz} \\ \tau_{yx} & \sigma_y & \tau_{yz} \\ \tau_{zx} & \tau_{zy} & \sigma_z \end{bmatrix} \mathbf{T}^T \tag{19}$$

where $\mathbf{T}$ is the direction cosine matrix. The stress–strain relations in the unified material system are presented in Fig. 7. The maximum effective strain for each model in Table 2 is calculated at the successive time step after the failure of the fibres takes place. The models C00, C15, C30, C45, C60 reach the strength in fibre direction (Fig. 7 (a)) and fail due to the failure of fibres. The failure of the model is complete as the matrix fails at the same time as fibres which results in the drop-off of the stresses in the transverse direction (Fig. 7(b)). The matrix material for the model C75 fails before the failure of the fibres take place and this results in significantly higher ERODS value compared with the ERODS values calculated for the models discussed previously. Moreover, the fibres do not fail for the material model C90 which is equivalent to transverse tensile loading. The artificial ERODS value 5 represents this model in numerical examples.

3. Model verification by numerical examples

The impact of sphere at medium initial velocity (440 m/s) to the UDLT is analysed in numerical examples. Two models of the UDLT are considered. Solid element model of UDLT (Fig. 8(a)) is referred as a base model and represents the internal structure of the composite. The parameters of component materials match the parameter values in Table 1 used in evaluation of equivalent material characteristics. The mesh of solid model is coarser than the mesh
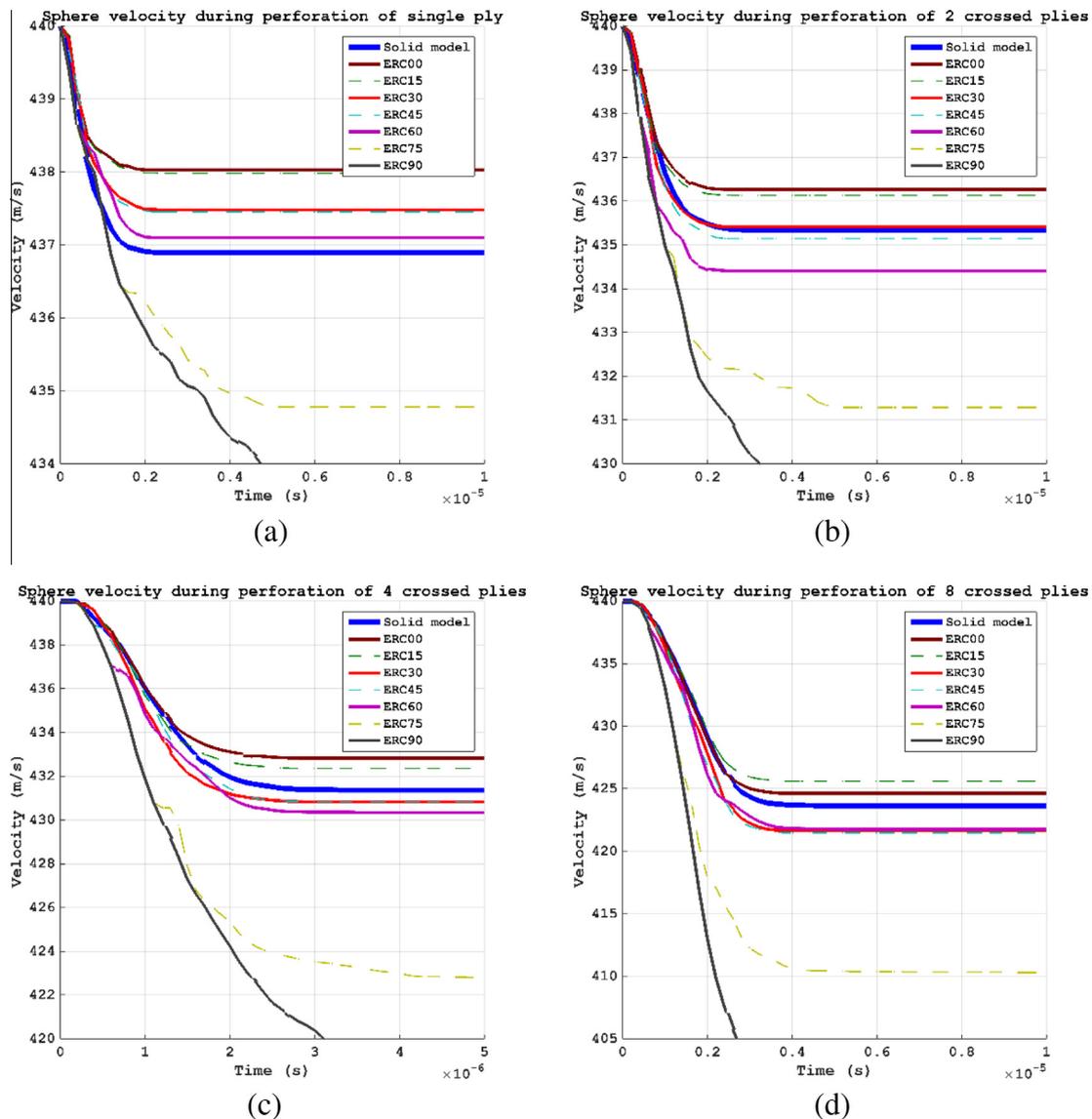

Fig. 9. Comparison of the sphere velocity during perforation of single ply (a) and 2 (b), 4 (c), 8 (d) crossed plies using solid-element model and shell models with ERODS values obtained using respective models for evaluation.

used for RVE in evaluation of parameters which may result in slightly reduced stiffness of the structure. Shell element models (Fig. 8(b)) with material parameters in Table 3 and ERODS values in Table 2 are analysed to identify the appropriate ERODS value for the impact of sphere. Factors SLIMS, SLIMTi, SLIMCi in Table 4 are applied to limit the strength values after the failure point is reached. If factors are equal to 1, the stress remains at a maximum value identical to the strength. This value is preferred for compressive and shear behaviour [14]. If the failure point is reached, the respective stress of the element is reduced to SLIMii*strength despite the strain value. One through-thickness integration point is employed for the shell element as the bending of shell is not considered. The sphere is modelled by shell elements as a rigid body. The material model *MAT_RIGID (MAT_020) is employed to define sphere material with the parameters in Table 4. All displacements in X and Y directions and all rotations are constrained for the nodes of sphere. The translational mass of sphere is equal to the mass of solid sphere with mass density in Table 4. The CONTACT_EROD ING_SURFACE_TO_SURFACE type is employed to define the contact interaction between the sphere and UDLT sheets. The same contact type is used for the contact interaction between the adjacent sheets of the models. On the contrary to other contact types in LS-DYNA, the contact surface for the eroding contact type is updated during the contact interaction. The models are reduced to the quarter with the appropriate symmetry conditions. In order to avoid failure of fibres due to the boundary effects, the material in marginal zone has significantly higher erosion values.

The change in sphere velocity during the perforation of the single ply of UDLT (Fig. 8(a)), two (Fig. 8(b)), four (Fig. 8(c)) and eight (Fig. 8(d)) crossed plies for mezzo-scale models with different ERODS values is compared with the change in sphere velocity for the respective model represented by 3D solid elements as a reference model. Sphere velocity of shell models can be classified to three groups. The first group represents shell models with ERODS values calculated for the material samples where matrix failure occurs before the fibre failure. Shell models ERC75 and ERC90 with ERODS values representing models C75 and C90 are significantly stiffer than other shell models and solid model. The second group consists of shell models ERC00 and ERC15 that exhibit brittle behaviour and sphere velocity is not reduced enough compared to the solid model. Results for sphere velocity with shell models of the third group ERC30, ERC45 and ERC60 converge as the number of plies is increased. The ERC60 model has the highest ERODS value and this value should be applied in successive calculations to ensure that elements are not eroded prematurely (see Fig. 9).

The radius of sphere in proportion to the radius of the fibre in solid element model is rather small and failure of each fibre has a significant influence in the sphere velocity. The deletion of shell element in the shell model has a significant effect likewise. To reduce the influence of single fibre or single shell element, the ratio of sphere radius to fibre radius should be increased and the larger models should be analysed. However, analysis of larger solid model is limited by computational resources.

4. Conclusions

Numerical simulation of composite materials with respect to the internal structure requires high computational resources. Moreover, the management of results takes unreasonable amount of time. The application of multi-scale models is a solution that enables to save computational time and resources.

The bridging between the micro and mezzo scales was analysed in this research. The complex internal structure of a single layer of composite material is analysed in micro scale. The equivalent linear elastic parameters and material strength are evaluated for the sample of typical material structure. Further on, the method to evaluate the effective strain for eroding shell element is introduced in this article. The method consists of applying longitudinal tensile load for the sample of rotated material structure. The equivalent stiffness and failure parameters obtained in this investigation have been verified by comparing the results of FE analysis of the models obtained in two different scales. As a reference model, the transverse impact of a rigid body to a composite sheet consisting of several plies presented in the micro-scale by 3D solid elements in LS-DYNA has been used. The adequacy of the results obtained by the FE analysis of much rougher mezzo-scale models based on the obtained equivalent stiffness and failure parameters with variety of erosion strain values has been estimated by comparison with the reference model results. The recommended ERODS value in successive calculation is the highest effective strain value calculated for the material sample where the failure of fibres take place before the failure of the matrix. This is caused by the fact that the failure of the matrix drastically increase the value of the effective strain. It should be noticed that the angle between the material coordinate system and the coordinate system the load is applied depends on the parameters of consisting materials and the internal structure. Furthermore, the application of ERODS value should be considered with respect to the specific problem. In addition, each unidirectional ply of the reference model corresponded to the single homogeneous orthotropic ply of the shell model in the research. For the more generalised model in the macro scale further research should be carried out, where integral behaviour of all plies should be presented by using continuous shell or volumetric finite elements and equivalent erosion strains should be evaluated with respect to the fibre direction in the constituent plies and by taking into account the contact interaction between the layers.

References

[1] Barauskas R, Abraitiene A. Computational analysis of impact of a bullet against the multilayer fabrics in LS-DYNA. Int J Impact Eng 2007;34:1286–305. http://dx.doi.org/10.1016/j.ijimpeng.2006.06.002.
[2] Nilakantan G, Keefe M, Bogetti TA, Gillespie JW. Multiscale modeling of the impact of textile fabrics based on hybrid element analysis. Int J Impact Eng 2010;37:1056–71. http://dx.doi.org/10.1016/j.ijimpeng.2010.04.007.
[3] Zhang C, Binienda WK, Goldberg RK, Kohlman LW. Meso-scale failure modeling of single layer triaxial braided composite using finite element method. Compos A Appl Sci Manuf 2014;58:36–46. http://dx.doi.org/10.1016/j.compositesa.2013.11.009.
[4] Younes R, Hallal A, Fardoun F, Chehade FH. Comparative review study on elastic properties modeling for unidirectional composite materials. In: Hu N, editor. InTech; 2012. Doi: http://dx.doi.org/10.5772/50362.
[5] Vasiliev VV, Morozov EV. Advanced mechanics of composite materials. Elsevier; 2007.
[6] Ernst G, Vogler M, Hühne C, Rolfes R. Multiscale progressive failure analysis of textile composites. Compos Sci Technol 2010;70:61–72. http://dx.doi.org/10.1016/j.compscitech.2009.09.006.
[7] Zhang C, Binienda WK. A meso-scale finite element model for simulating free-edge effect in carbon/epoxy textile composite. Mech Mater 2014;76:1–19. http://dx.doi.org/10.1016/j.mechmat.2014.05.002.
[8] Sun CT, Vaidya RS. Prediction of composite properties from a representative volume element. Compos Sci Technol 1996;56:171–9. http://dx.doi.org/10.1016/0266-3538(95)00141-7.
[9] Xia Z, Zhang Y, Ellyin F. A unified periodical boundary conditions for representative volume elements of composites and applications. Int J Solids Struct 2003;40:1907–21. http://dx.doi.org/10.1016/S0020-7683(03)00024-6.
[10] Kanit T, Forest S, Galliet I, Mounoury V, Jeulin D. Determination of the size of the representative volume element for random composites: statistical and numerical approach. Int J Solids Struct 2003;40:3647–79. http://dx.doi.org/10.1016/S0020-7683(03)00143-4.

[11] Burgoyne CJ. Aramid fibres for civil engineering applications. In: Construction material reference book. Butterworth-Heinemann; 1992.

[12] Barauskas R, Abraitiene A. Multi-resolution finite element models for simulation of the ballistic impact on non-crimped composite fabric packages. Compos Struct 2013;104:215–29. http://dx.doi.org/10.1016/j.compstruct.2013.04.014.

[13] Zhang B, Yang Z, Sun X, Tang Z. A virtual experimental approach to estimate composite mechanical properties: modeling with an explicit finite element method. Comput Mater Sci 2010;49:645–51. http://dx.doi.org/10.1016/j.commatsci.2010.06.007.

[14] LS-DYNA Keyword User's Manual, vol. I. Livermore Software Technology Corporation; 2007.

[15] Schweizerhof K, Weimar K, Munz T, Rottner T. Crashworthiness analysis with enhanced composite material models in LS-DYNA – merits and limits. In: 5th International LS-DYNA Users Conference. 1998.

[16] Maimí P, Camanho PP, Mayugo JA, Dávila CG. A continuum damage model for composite laminates: Part II – computational implementation and validation. Mech Mater 2007;39:909–19. http://dx.doi.org/10.1016/j.mechmat.2007.03.006.